Beam Design for Beam Switching Based Millimeter Wave Vehicle-to-Infrastructure Communications

Vutha Va*, Takayuki Shimizu†, Gaurav Bansal†, and Robert W. Heath Jr.*
*Wireless Networking and Communications Group, The University of Texas at Austin
Email: vutha.va@utexas.edu, rheath@utexas.edu
†TOYOTA InfoTechnology Center, U.S.A., Inc., Mountain View, CA
Email: tshimizu@us.toyota-itc.com, gbansal@us.toyota-itc.com

***Abstract*—Beam alignment is a source of overhead in mobile millimeter wave communication systems due to the need for frequent repointing. Beam switching architectures can reduce the amount of repointing required by leveraging position prediction. This paper presents an optimization of beam design in terms of rate. We consider a non-congested two-lane highway scenario where road side units are installed on lighting poles. Under this scenario, line-of-sight to the road side unit is very likely and vehicle speed does not vary much. We formulate and solve numerically using a gradient descent method for an optimal beam design to maximize the data rate for non-overlap beams. The result shows close performance to the equal coverage beam design. We study the effect of the overlap on the average rate and outage and compare the equal coverage with the equal beamwidth design. Numerical examples show that the equal coverage design can achieve up to 1.5x the rate of the equal beamwidth design confirming the importance of the choice of beam design.**

I. Introduction

Vehicles are gradually incorporating more sensing capabilities in an effort towards safer and more automated driving [1]. Sensing data could be shared with neighbor vehicles for data fusion [2], or with the road side unit (RSU) to take advantage of an efficient cloud computing infrastructure [3]. Vehicles can also benefit from digital maps which can complement with the sensing data [4]. To enable these applications, Gbps data rate is required. Unfortunately, the current Dedicated Short-Range Communication (DSRC) standard can support only up to 27 Mbps [5]. Millimeter wave (mmWave) bands with larger spectral channels have the ability to meet the need for high data rates [6]. Due to its propagation characteristics, beamforming is required to provide sufficient link quality [7]. Thus to enable mmWave vehicle-to-infrastructure (V2I) communications, an efficient beamforming method that can adapt to the vehicular speed is required.

This paper optimizes the beams in a mmWave V2I network where beam switching based on position prediction is employed. Beamforming is important in mmWave systems as the array gain compensates for the small antenna aperture and the large noise bandwidth [7]. In mobile systems, however, beamforming is a source of system overhead as frequent updates are required to repoint the beam. An alternative is to employ a switched beam system, where the beams are successively switched over time. Leveraging the feedback from the vehicle via a lower band (e.g., DSRC), the switching timing can be computed and the lengthy beam training used in conventional beam sweeping [8] is not required. We consider a two-lane highway scenario where the RSUs are mounted on lighting poles. It is argued that line-of-sight (LOS) is very likely and in that case position is enough for aligning the beams. The performance though is limited by the position prediction error which can be mitigated using overlapping beams. We formulate a beam design problem to maximize the rate for the non-overlap case, which can be perturbed to introduce the overlap without much change in the rate. The optimization is solved using a gradient descent method, and the solution shows very close performance to the equal coverage design. We study the effect of overlap on the average rate and outage. Comparing the equal coverage and the equal beamwidth design, shows that the gain in average rate can be up to 1.5x over the equal beamwidth case. Our results provide insights into the width of the beams and the extent of overlap that should be employed.

Prior has considered mmWave for V2I in several different contexts. A radio-on-fiber (RoF) based system was proposed in [9], where multiple RSUs are grouped and controlled by a control station. These RSUs transmit simultaneously on the same band and code division multiplexing was used to manage interference in overlap regions. Our work uses position prediction to switch the beams in time and thus does not have such interference. More recently, [10] studies several handover algorithms for a 60 GHz RoF V2I network. These algorithms do not use position prediction and handover is triggered by beacon signals. Our architecture leverages position prediction and does not require handover among the beams. Handover between RSUs, although not considered in this work, could leverage DSRC and/or position prediction. Also, our architecture allows the use of narrow beams and can have larger RSU spacing which can reduce infrastructure cost compared to prior solution. Similar architecture to ours has been studied in a train context in [11] where the authors optimized the frequency to perform beam sweeping to avoid misalignment. In our previous work [12], we evaluated the average rate for the equal beamwidth design without overlap while this work optimizes the beam design and allows overlap between beams.

II. MmWave V2I with Beam Switching

Consider a highway scenario where a network of RSUs is installed along the roadside. The passing vehicle wants to

978-1-4799-6664-6/16/$31.00 ©2016 IEEE

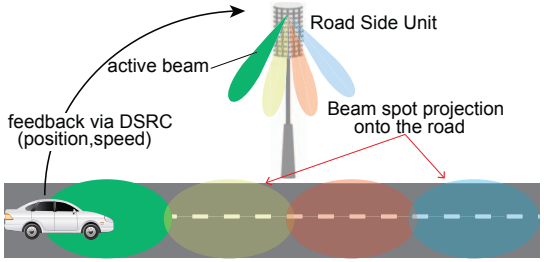

(a) At time t_0

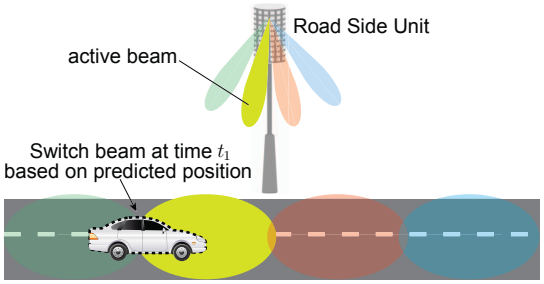

(b) At time t_1

Fig. 1. Beam alignment based on beam switching.

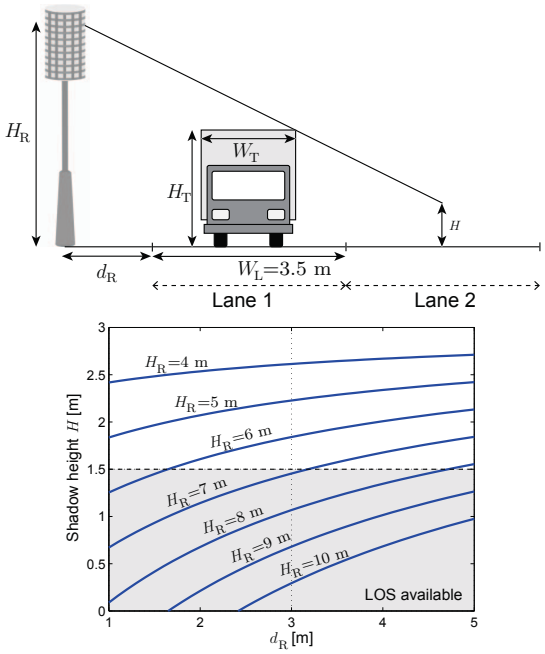

Fig. 2. Two-lane highway scenario with potential blockage by a truck. The top illustration shows the geometry of the blockage scenario and the plots show the shadow heights at the center of Lane 2 as a function of d_R for different H_R. $H_T = 3$ m, $W_T = 2.4$ m, and $W_L = 3.5$ m are used.

communicate with the RSU over a mmWave link. MmWave requires beamforming to compensate for the high path loss. Thus, the beam pointing direction needs to be aligned at all time to maintain link quality. Conventional approaches for beam alignment are based on beam sweeping [8], which have high beam training overhead and do not make use of the sensors in the vehicle. Here we consider an efficient beam alignment method based on beam switching that takes advantage of vehicle position information [12].

Fig. 1 illustrates the proposed beam switching solution. At time t_0 when the vehicle enters the coverage of the RSU, it feeds back its position and speed at that time to the RSU using DSRC. Depending on the accuracy of the position information, a refine beam alignment might be required at this initial stage to reduce the position uncertainty. This is basically a beam sweeping with very narrow beams. We pointed out in [12] that Doppler effect could render feedback over mmWave link impossible and is a potential point of failure for beam sweeping. Here the feedback is over the DSRC link at a much lower carrier frequency and thus there is no such problem. Once the initial position is known, the vehicle trajectory can be predicted from the speed feedback. For example, in Fig 1(b) it is predicted from the feedback that the vehicle will enter the coverage of the second beam at time t_1 and thus the beam should be switched from the first to the second at t_1. This is done similarly for subsequent beams. Note that here only one initial feedback (and refine beam alignment if position error is large) is required which greatly reduces the overhead. The prediction error will grow in time due to the speed error and thus it might be desirable to feedback multiple times to suppress the prediction error. In the analysis in Section IV, we consider the worst case where only one feedback is used.

III. Models and Assumptions

We consider a two-lane highway scenario where RSUs are mounted on lighting poles. Under this setting, justification for the LOS link between the RSU and the vehicle is provided. Next, the mobility and the link budget model are described.

A. Line of Sight Availability

For the two-lane highway scenario, blockage can happen only when there is a large vehicle in Lane 1 and the target vehicle is in Lane 2. Fig. 2 illustrates this case with a truck as the potential blocker. The shadow height at the middle of Lane 2 can be computed from the geometry and is given as

$$H(H_R, d_R) = H_T - \frac{W_L - W_T/2}{d_R + \frac{1}{2}(W_L + W_T)}(H_R - H_T). \quad (1)$$

If the shadow height is smaller than the target vehicle's height, then LOS is available. Assuming a typical car's height of 1.5 m, and set $H_T = 3$ m, $W_T = 2.4$ m, and $W_L = 3.5$, then the LOS region is the shaded area in Fig. 2. In typical cases, the lighting poles distance to Lane 1 is less than 3 m and the typical lighting pole height is around 25 feet (7.62 m), we conclude that LOS is very likely and is assumed in this work.

B. Mobility Model

This work assumes the vehicle is traveling at constant speed during the entire time under the coverage of an RSU ($\sim$100 m order). This constant speed model corresponds to the free flow traffic condition [13]. The vehicle feeds back its position and speed along with the time stamp to the RSU via DSRC when it first enters the coverage. It is assumed that beam sweeping

is conducted if necessary, so that the feedback position x_0 and time stamp t_0 have negligible error. Estimated speed is assumed to be affected by addictive Gaussian error, i.e.,

$$\hat{v} = v + v_{\mathrm{e}}, \tag{2}$$

where v is the actual speed and $v_{\mathrm{e}} \sim \mathcal{N}(0, \sigma_v^2)$ is Gaussian with zero mean and variance of σ_v^2. The position of the vehicle is predicted using the feedback speed estimate, i.e.,

$$x(t) = (t - t_0)\hat{v} + x_0. \tag{3}$$

Without loss of generality, we set $t_0 = 0$ and $x_0 = 0$.

C. Link Budget Model

We assume analog beamforming at both the RSU and vehicle which control the beams digitally using phase shifters. No constraint on the antenna size is assumed. This is a subject of our future work which emphasizes the difference between the uplink and downlink as the antenna size is more constrained at the vehicle side. Under LOS conditions, the receive power is given by [11], [14]

$$P_{\mathrm{rx}}^{\mathrm{dBm}} = P_{\mathrm{tx}}^{\mathrm{dBm}} + G_{\mathrm{tx}} + G_{\mathrm{rx}} - W + 10n \log_{10} \frac{\lambda}{4\pi d}, \tag{4}$$

where $P_{\mathrm{tx}}^{\mathrm{dBm}}$ and $P_{\mathrm{rx}}^{\mathrm{dBm}}$ are the transmit and receive power, G_{tx} and G_{rx} are the transmit and receive antenna gains in dB, W is the shadowing margin in dB to account for weather conditions such as rain, n is the path loss exponent, λ is the carrier wavelength, and d is the distance from the RSU. For simplicity, here transmission with constant EIRP (Effective Isotropically Radiated Power) is assumed and the receive power in linear scale can be written as

$$P_{\mathrm{rx}}(t, \theta_{\mathrm{b}}) = \frac{A\, G_{\mathrm{rx}}(\theta_{\mathrm{b}})}{[(vt - d_\ell/2)^2 + d_{\mathrm{ele}}^2]^{n/2}}, \tag{5}$$

where $10 \log_{10}(A) = \mathsf{EIRP}_{\mathrm{dBm}} - W + 10n \log_{10} \frac{\lambda}{4\pi}$, θ_{b} the receive beamwidth, d_ℓ the coverage length of the RSU, and $d_{\mathrm{ele}}^2 = d_0^2 + (H_{\mathrm{R}} - H_{\mathrm{V}})^2$ with d_0 as shown in Fig. 3, H_{R} the RSU height, and H_{V} the vehicle height.

An ideal beam with constant gain and zero sidelobe is assumed. The antenna gain can then be approximated by [15]

$$G_{\mathrm{rx}}(\theta_{\mathrm{b}}) \simeq \frac{\pi^2}{\theta_{\mathrm{ele}} \theta_{\mathrm{b}}}, \tag{6}$$

where θ_{ele} is the beamwidth in the elevation plane. In this work, θ_{ele} is fixed such that the resulting beam covers the width of the two lanes. For $d_0 = 3$ m, $\theta_{\mathrm{ele}} = 31^\circ$.

IV. Average Rate and Outage

This section derives the average rate and outage for a given beam design. Fig. 3 shows a beam design with three overlapping beams. The coverage of the i-th beam is the interval $[b_{i,\mathrm{b}}, b_{i,\mathrm{e}}]$. Since we assume the error has zero mean, the switching timing should be chosen as the middle point in the overlap region, i.e., the mid-point of $[b_{i+1,\mathrm{b}}, b_{i,\mathrm{e}}]$. For example, the first beam should be switched to the second one at the time that the vehicle is predicted to arrive at the middle point of $[b_{2,\mathrm{b}}, b_{1,\mathrm{e}}]$ which is denoted by b_1 in Fig. 3.

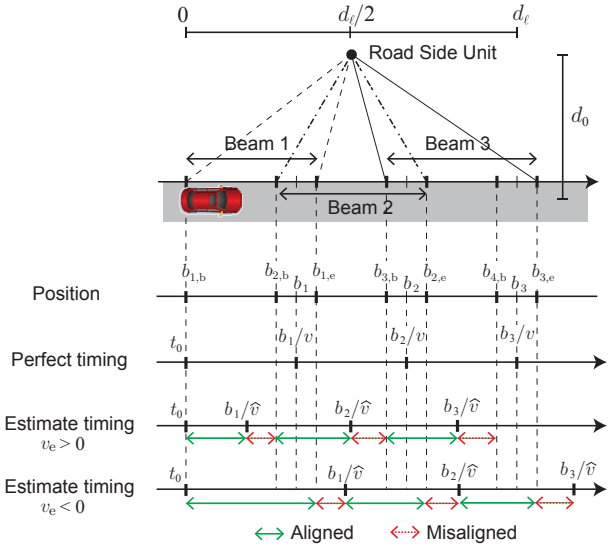

Fig. 3. Beam design and switching timing. The top figure shows a top view of a network with three overlapping beams in the coverage. The bottom part shows the perfect switching timing and how misalignment can happen when the speed estimate has error.

A. Average Rate

Using the switching timing as described above, the average rate can now be derived. For the instantaneous rate the Shannon capacity formula is used, i.e., $r(t, \theta_{\mathrm{b}}) = \log(1 + \rho(t, \theta_{\mathrm{b}}))$, where $\rho(t, \theta_{\mathrm{b}}) = P_{\mathrm{rx}}(t, \theta_{\mathrm{b}})/P_{\mathrm{n}}$ is the instantaneous SNR. To compute the average rate, $r(t, \theta_{\mathrm{b}})$ has to be integrated over the duration that the beams are aligned. This is because of the assumption of the idealized beam where the gain outside the beamwidth is zero and thus the rate is zero when misaligned. The perfect timing to switch from the i-th beam to the $(i+1)$-th beam is b_i/v, but this timing is not known and the best guest is $b_i/\hat{v}$. Depending on the speed estimation error, the switching timing can be too fast or too slow as shown in Fig. 3. The overlap provides a protection region so that misalignment will not happen for small $|v_{\mathrm{e}}|$. If $|v_{\mathrm{e}}|$ is large so that the actual position at the predicted switching timing is outside the overlap region, misalignment will happen. To simplify the computation, it is divided into two cases, i.e., when $v_{\mathrm{e}} \geq 0$ and when $v_{\mathrm{e}} < 0$. Using the diagram in Fig. 3, the total amount of data received in the i-th beam can be written as

$$D_i(\boldsymbol{\theta} | v_{\mathrm{e}} \geq 0) = B \int_{\max\left\{\frac{b_{i,\mathrm{b}}}{v}, \frac{b_{i-1}}{v+v_{\mathrm{e}}}\right\}}^{\frac{b_i}{v+v_{\mathrm{e}}}} \log(1 + \rho(t, \theta_i))\mathrm{d}t, \tag{7}$$

$$D_i(\boldsymbol{\theta} | v_{\mathrm{e}} < 0) = B \int_{\frac{b_{i-1}}{v+v_{\mathrm{e}}}}^{\min\left\{\frac{b_{i,\mathrm{e}}}{v}, \frac{b_i}{v+v_{\mathrm{e}}}\right\}} \log(1 + \rho(t, \theta_i))\mathrm{d}t, \tag{8}$$

where $\boldsymbol{\theta} = [\theta_1, \theta_2, \ldots, \theta_{N_{\mathrm{b}}}]$ with θ_i the beamwidth of the i-th beam and N_{b} the number of beams in the coverage, and B is the system bandwidth. Note that knowing d_0 and d_ℓ, $\boldsymbol{\theta}$ contains all the information to compute the beam boundaries. When the speed error is too large, the beam can be missed the whole time. This happens when $b_{i,\mathrm{b}}/v > b_i/(v + v_{\mathrm{e}})$ and

$b_{i-1}/(v+v_\mathrm{e}) > b_{i,\mathrm{e}}/v$ for the case when $v_\mathrm{e} \geq 0$ and $v_\mathrm{e} < 0$, respectively. The condition in terms of v_e becomes

$$\begin{cases} v_\mathrm{e} > \frac{b_i - b_{i,\mathrm{b}}}{b_{i,\mathrm{b}}} & \text{if } v_\mathrm{e} \geq 0 \\ v_\mathrm{e} < \frac{b_{i-1} - b_{i,\mathrm{e}}}{b_{i,\mathrm{e}}} & \text{if } v_\mathrm{e} < 0 \end{cases}. \tag{9}$$

Incorporating (9), the average rate can be written as

$$\begin{aligned} R_i(\boldsymbol{\theta}) = &\int_0^{\frac{b_i - b_{i,\mathrm{b}}}{b_{i,\mathrm{b}}} v} \frac{v + v_\mathrm{e}}{d_\ell} D_i(\boldsymbol{\theta} | v_\mathrm{e} \geq 0) f_{v_\mathrm{e}}(v_\mathrm{e}) \mathrm{d}v_\mathrm{e} \\ &+ \int_{\frac{b_{i-1} - b_{i,\mathrm{e}}}{b_{i,\mathrm{e}}} v}^{0} \frac{v + v_\mathrm{e}}{d_\ell} D_i(\boldsymbol{\theta} | v_\mathrm{e} < 0) f_{v_\mathrm{e}}(v_\mathrm{e}) \mathrm{d}v_\mathrm{e}, \end{aligned} \tag{10}$$

where $f_{v_\mathrm{e}}(\cdot)$ denotes the probability density function of v_e.

Note that the above result includes the non-overlap case as a special case which was studied in our previous work [12]. In particular, the non-overlap case corresponds to the case when $b_{i,\mathrm{b}} = b_{i-1,\mathrm{e}} = b_{i-1}$. Also as noted in [14], the LOS case can be approximated by a free space loss with the path loss exponent $n = 2$. In that case, $D_i(\boldsymbol{\theta})$ can be computed analytically. For the non-overlap case with zero speed error, the expression can be written as

$$\begin{aligned} &D_i(\boldsymbol{\theta}) = \\ &\frac{-1}{2v} \left[(d_\ell - 2b_{i+1}) \log\left(1 + \rho\left(\frac{b_{i+1}}{v}, \theta_i\right)\right) + 4\sqrt{\frac{a}{\theta_i} + d_{\mathrm{ele}}^2} \cdot \right. \\ &\left. \tan^{-1}\left(\frac{d_\ell/2 - b_{i+1}}{\sqrt{\frac{a}{\theta_i} + d_{\mathrm{ele}}^2}}\right) - 4 d_{\mathrm{ele}} \tan^{-1}\left(\frac{d_\ell/2 - b_{i+1}}{d_{\mathrm{ele}}}\right) \right] \\ &+ \frac{1}{2v} \left[(d_\ell - 2b_i) \log\left(1 + \rho\left(\frac{b_i}{v}, \theta_i\right)\right) + 4\sqrt{\frac{a}{\theta_i} + d_{\mathrm{ele}}^2} \cdot \right. \\ &\left. \tan^{-1}\left(\frac{d_\ell/2 - b_i}{\sqrt{\frac{a}{\theta_i} + d_{\mathrm{ele}}^2}}\right) - 4 d_{\mathrm{ele}} \tan^{-1}\left(\frac{d_\ell/2 - b_i}{d_{\mathrm{ele}}}\right) \right]. \end{aligned} \tag{11}$$

This result will be used in Section V on beam design.

B. Outage

The outage here is defined as the duration of misalignment averaged over the speed estimation error. This can be computed from the diagram in Fig. 3. One thing to be careful in this computation is that the misaligned duration cannot be larger than the time in the coverage of the beam. Taking that into account, the outage for the i-th beam can be written as

$$\begin{aligned} T_{\mathrm{out},i}(\boldsymbol{\theta} | v_\mathrm{e} \geq 0) = &\frac{b_{i+1,\mathrm{b}} - b_{i,\mathrm{b}}}{v} Q\left(\frac{b_i - b_{i,\mathrm{b}}}{b_{i,\mathrm{b}}} \frac{v}{\sigma_v}\right) \\ &+ \int_{\frac{b_i - b_{i+1,\mathrm{b}}}{b_{i+1,\mathrm{b}}} v}^{\frac{b_i - b_{i,\mathrm{b}}}{b_{i,\mathrm{b}}} v} \left(\frac{b_{i+1,\mathrm{b}}}{v} - \frac{b_i}{v + v_\mathrm{e}}\right) f_{v_\mathrm{e}}(v_\mathrm{e}) \mathrm{d}v_\mathrm{e}, \end{aligned} \tag{12}$$

$$\begin{aligned} T_{\mathrm{out},i}(\boldsymbol{\theta} | v_\mathrm{e} < 0) = &\frac{b_{i,\mathrm{e}} - b_{i-1,\mathrm{e}}}{v} Q\left(\frac{b_{i,\mathrm{e}} - b_{i-1}}{b_{i,\mathrm{e}}} \frac{v}{\sigma_v}\right) \\ &+ \int_{\frac{b_{i-1} - b_{i,\mathrm{e}}}{b_{i,\mathrm{e}}} v}^{\frac{b_i - b_{i,\mathrm{e}}}{b_{i,\mathrm{e}}} v} \left(\frac{b_i}{v + v_\mathrm{e}} - \frac{b_{i,\mathrm{e}}}{v}\right) f_{v_\mathrm{e}}(v_\mathrm{e}) \mathrm{d}v_\mathrm{e}, \end{aligned} \tag{13}$$

TABLE I
LIST OF PARAMETERS USED IN NUMERICAL EXAMPLES

Parameter		Value
Path loss exponent	n	2
Carrier frequency	f_c	60 GHz
Bandwidth	B	2.16 GHz
Shadowing margin	W	10 dB
(see Fig. 3)	d_0	3 m
(see Fig. 3)	d_ℓ	100 m
RSU height	H_R	7 m
Vehicle height	H_V	1.5 m
Vehicle speed	v	30 m/s
Noise figure	NF	6 dB
Noise power	P_n	$-174 + 10\log_{10} B + \mathsf{NF}$ dBm
Effective Isotropically Radiated Power	EIRP	20 dBm

where $Q(\cdot)$ is the Q-function. The first term in (12) corresponds to the case when $v_\mathrm{e} > \frac{b_i - b_{i,\mathrm{b}}}{b_{i,\mathrm{b}}}$, i.e., when v_e is too large so that the beam is misaligned the whole time. The probability that this happens can be expressed using the Q-function because v_e is Gaussian. The second term in (12) integrates from $\frac{b_i - b_{i+1,\mathrm{b}}}{b_{i+1,\mathrm{b}}} v$ instead of zero reflecting the effect of overlap which can absorb small prediction error. Similar interpretation applies to (13). For speed error with σ_v on the order of a few percent of v, the first terms in (12) and (13) are negligible since the Q-function will become very small.

V. Beam Design

This section investigates how to design the beams to maximize the data rate. First, we provide some evidence showing that the equal coverage beam design is near-optimal. Then we study the rate and outage versus the overlap ratio.

The rate optimization problem can be expressed as

$$\underset{\boldsymbol{\theta}}{\text{maximize}} \quad \sum_{i=1}^{N_\mathrm{b}} R_i(\boldsymbol{\theta}) \tag{14}$$

$$\text{subject to} \quad \theta_1 + \theta_2 + \cdots + \theta_{N_\mathrm{b}} = \theta_{\mathrm{RSU}} \tag{15}$$

$$\theta_i > 0, \quad i = 1, 2, \ldots, N_\mathrm{b} \tag{16}$$

where θ_{RSU} is the angular coverage of the RSU. In this general setting, the optimization is over all possible N_b, the dimension of $\boldsymbol{\theta}$. Instead of solving this problem directly, here it is relaxed by fixing N_b. The rational for this relaxation is this. If the solution for a given N_b is known, one can find the optimal N_b by repeating the calculation over different N_b and compare. This is possible because N_b is discrete. As can be seen in (10), $R_i(\boldsymbol{\theta})$ is a complicated function involving an integration whose interval also depends on $\boldsymbol{\theta}$. We further relax the problem to consider the non-overlap case with negligible speed error and avoid the integration in (10). This relaxation does not affect the essence of the beam design because the estimation error can be mitigated with the overlap and the difference between the overlap and non-overlap case is in the broadening of the beamwidth which has similar effect for any beam design with the same overlap size. For simplicity, here N_b is assumed to be even so that symmetry can be used and only half of the

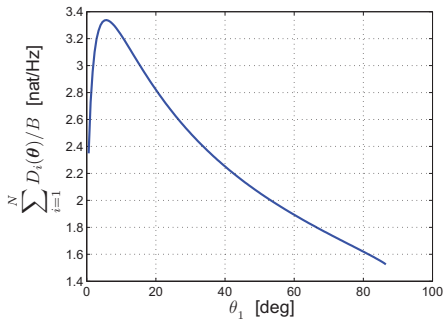

(a) $\sum_{i=1}^{N} D_i(\boldsymbol{\theta})/B$ for $N = 2$

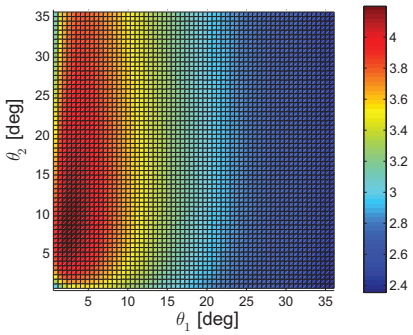

(b) $\sum_{i=1}^{N} D_i(\boldsymbol{\theta})/B$ for $N = 3$

Fig. 4. Total receive data for the case when $N = 2$ and $N = 3$. $\sum_{i=1}^{N} D_i(\boldsymbol{\theta})$ is a function of $N-1$ variables when plugging in the constraint in (18), and thus for $N = 2$ and $N = 3$, it is a one and two dimensional function, respectively. For $N = 2$, it can be observed that the function is concave near the peak but is convex at the vicinity of $\theta_1 = 40°$. For both $N = 2$ and $N = 3$, there is only one peak. The parameters used are shown in Table I.

coverage needs to be considered. With these relaxations, the optimization problem now can be expressed as

$$\underset{\boldsymbol{\theta}}{\text{maximize}} \quad \sum_{i=1}^{N} D_i(\boldsymbol{\theta}) \tag{17}$$

$$\text{subject to} \quad \theta_1 + \theta_2 + \cdots + \theta_N = \theta_0 \tag{18}$$

$$\theta_i > 0, \quad i = 1, 2, \ldots, N \tag{19}$$

where $D_i(\boldsymbol{\theta})$ is as given in (11), $N = N_\mathrm{b}/2$, $\theta_0 = \theta_\mathrm{RSU}/2$, and we abuse the notation a bit by using the same $\boldsymbol{\theta}$ as before although here it only has half the size. Note that the objective function now is in terms of $D_i(\boldsymbol{\theta})$ instead of $R_i(\boldsymbol{\theta})$, which are equivalent as the objective function because the two are related by a constant factor when speed error is neglected. The last piece that is needed to complete the problem is the relation between the beamwidth and the beam boundaries which can be computed from the geometry and is given by

$$b_i = \frac{d_\ell}{2} - d_0 \tan\left(\theta_0 - \sum_{k=1}^{i} \theta_k\right), \qquad i = 1, 2, \ldots, N. \tag{20}$$

The problem in (17), unfortunately, is not convex because the objective function $\sum_{i=1}^{N} D_i(\boldsymbol{\theta})$ is neither convex nor concave (see Fig. 4). As evident from (11), the function is smooth. For $N = 2$ and $N = 3$ case, there is only one peak.

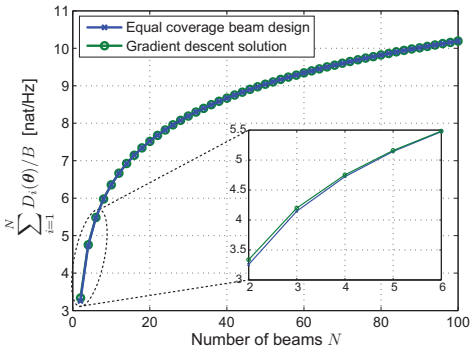

Fig. 5. Comparison of the solution from the gradient descent and that of the equal coverage beam design. The parameters used are shown in Table I. The equal coverage beam design performs slightly worse for small N but the difference becomes indistinguishable for $N \geq 5$.

With these observations, it is conjectured that the objective has only one peak and a gradient descent with backtracking line search [16] is applied. As gradient descent always moves in the increasing value of the objective, it will reach the peak from any starting point. For fast convergence, however, a starting point near the optimal solution is preferable. The optimal solution should use a narrow beam to the edge because otherwise this beam will cover a wide area (property from the geometry) which suffers low gain. The beams are stretched less for smaller distances to the RSU, so this effect will be less for subsequent beams. This intuition tells us that the optimal solution should have beamwidths increasing from the edge toward the center, i.e., $\theta_1, \ldots, \theta_N$ should be in increasing order. The equal coverage design has this property and thus is chosen here. The gradient of $\sum_{i=1}^{N} D_i(\boldsymbol{\theta})$ can be computed in principle but becomes intractable as N grows. Instead, we use finite difference to approximate the gradient numerically. The stopping criterion is set to $\left\| \nabla_{\boldsymbol{\theta}} \left(\sum_{i=1}^{N} D_i(\boldsymbol{\theta}) \right) \right\| < 0.01$. The result is shown along with a comparison to the equal coverage design in Fig. 5. The gradient descent solution is slightly better for small N but becomes indistinguishable for $N \geq 5$. From this, we conclude that the equal coverage beam design is near-optimal in terms of maximizing the data rate.

Having shown that the equal coverage beam design performs well, now we provide some numerical examples showing its performance. Since outage is also an important metric, here we consider both the average rate and outage. The source of the outage is the beam misalignment due to the position prediction error, which can be mitigated by introducing overlap in the beam design. The overlap ratio is defined as the ratio of the overlap size to the beam itself. To demonstrate the effect of the beam design, the equal beamwidth beam design is compared with the equal coverage beam design. The overlap ratio definition for the two designs is a bit different: for the equal beamwidth case it is defined in terms of the overlap in angle while for the equal coverage beam design it is defined in terms of the coverage length. The difference in the definition is to allow a unified way to define the overlap for the comparison

between the two designs.

Fig. 6 shows the average rate and outage of the two designs as a function of the overlap ratio when the number of beams is fixed at $N_{\mathrm{b}} = 10, 20$, and 40. The parameters used are shown in Table I, and the speed error is set to $\sigma_v^2 = (0.01v)^2$. From Fig. 6(a), we can see that the outage decreases with the overlap ratio, but the two designs have different trends. The equal coverage design decreases faster than that of the equal beamwidth design. This is because the equal beamwidth design has wider beam coverage at the edge (geometrical property), and the overlap is large. This provides some tolerance to the position error and thus the low outage for small overlap ratios. Using the same beamwidth for the inner beams means that the coverages near the center are small and thus increasing the overlap ratio does not provide much protection there resulting in slow decrease with the overlap ratio. Fig. 6(b) shows the average rates for the same setting. By introducing overlap while keeping the number of beams fixed, the beamwidths widen resulting in lower gain and thus the decreases in the rate. If the target outage is 2% and $N_{\mathrm{b}} = 40$, then the equal coverage design requires overlap ratio of 0.7 and can achieve a rate of around 12 Gbps while the equal beamwidth design cannot achieve the outage and the rate is about 4 Gbps below the equal coverage design, i.e. the gain in rate is over 1.5x. Therefore, a proper choice of beam design is very important.

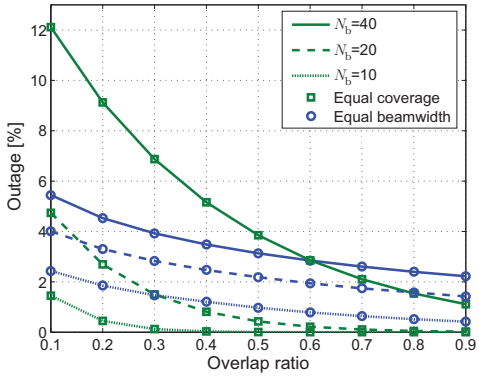

(a) Outage versus overlap ratios

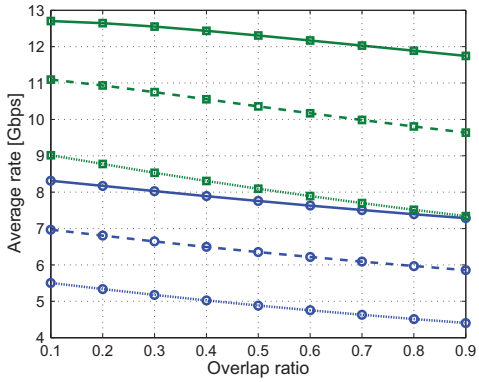

(b) Average rate versus overlap ratio

Fig. 6. Outage and average rate as functions of overlap ratios when the number of beams N_{b} is fixed. The parameters used are shown in Table I.

VI. Conclusions

This paper studied the beam design to maximize the data rate for a beam switching based mmWave V2I system. Using our derived expressions, we formulated an optimal beam design problem and the solution shows that the equal coverage beam design has negligible loss to the optimal one. This result agrees with the intuition that narrower beams should be used toward the edge where the coverage of a given beamwidth gets stretched out. We also showed how overlap affects the average rate and outage. The outage decreases with the overlap ratio but increases with the number of beams. In contrast, the average rate increases with the number of beams but decreases with the overlap ratio. The largest number of beams needed to maximize the rate is constrained by the outage target.

Acknowledgment

This research is supported in part by the U.S. Department of Transportation through the Data-Supported Transportation Operations and Planning (D-STOP) Tier 1 University Transportation Center and by a gift from TOYOTA Info Technology Center, U.S.A., Inc.

References

[1] N. Lu, *et al.*, "Connected vehicles: Solutions and challenges," *IEEE Internet Things J.*, vol. 1, no. 4, pp. 289–299, 2014.

[2] P. Tientrakool, Y.-C. Ho, and N. Maxemchuk, "Highway capacity benefits from using vehicle-to-vehicle communication and sensors for collision avoidance," in *IEEE VTC-Fall 2011*, Sep. 2011, pp. 1–5.

[3] F. Bonomi, R. Milito, J. Zhu, and S. Addepalli, "Fog computing and its role in the internet of things," in *ACM SIGCOMM*, 2012, pp. 13–16.

[4] J. Levinson, *et al.*, "Towards fully autonomous driving: Systems and algorithms," in *IEEE IV2011*, Jun. 2011, pp. 163–168.

[5] "IEEE std 802.11p-2010," *IEEE Standard*, pp. 1–51, Jul. 2010.

[6] T. S. Rappaport, *et al.*, "Millimeter wave mobile communications for 5G cellular: It will work!" *IEEE Access*, vol. 1, pp. 335–349, May 2013.

[7] T. S. Rappaport, R. W. Heath Jr., R. C. Daniels, and J. N. Murdock, *Millimeter Wave Wireless Communications*. Pearson, Sep. 2014.

[8] K. Hosoya, *et al.*, "Multiple sector ID capture (MIDC): A novel beamforming technique for 60-GHz band multi-Gbps WLAN/PAN systems," *IEEE Trans. Antennas Propag.*, vol. 63, no. 1, pp. 81–96, Jan. 2015.

[9] H. Harada, K. Sato, and M. Fujise, "A radio-on-fiber based millimeter-wave road-vehicle communication system by a code division multiplexing radio transmission scheme," *IEEE Trans. Intell. Transp. Syst.*, vol. 2, no. 4, pp. 165–179, 2001.

[10] N. D. Tselikas, E. A. Kosmatos, and A. C. Boucouvalas, "Performance evaluation of handoff algorithms applied in vehicular 60GHz radio-over-fiber networks," in *Proceedings of PM2HW2N '13*, 2013, pp. 161–166.

[11] J. Kim and A. F. Molisch, "Enabling Gigabit services for IEEE 802.11ad-capable high-speed train networks," in *IEEE Radio and Wireless Symposium (RWS), 2013*, Jan. 2013, pp. 145–147.

[12] V. Va, X. Zhang, and R. W. Heath Jr., "Beam switching for millimeter wave communication to support high speed trains," in *IEEE VTC-Fall 2015*, Sep. 2015.

[13] W. Knospe, L. Santen, A. Schadschneider, and M. Schreckenberg, "Single-vehicle data of highway traffic: Microscopic description of traffic phases," *Physical Review E*, vol. 65, no. 5, pp. 1–16, 2002.

[14] A. Yamamoto, *et al.*, "Path-loss prediction models for intervehicle communication at 60 GHz," *IEEE Trans. Veh. Technol.*, vol. 57, no. 1, pp. 65–78, Jan 2008.

[15] C. A. Balanis, *Antenna Theory: Analysis and Design*, 3rd ed. Wiley-Interscience, 2005.

[16] S. Boyd and L. Vandenberghe, *Convex Optimization*. New York, NY, USA: Cambridge University Press, 2004.